Outstanding Magneto-Caloric Effect of a $Gd_{60}Ni_{37}Co_3$ Amorphous Alloy *

Yan-Fei Ma(马雁飞), Ben-Zhen Tang(唐本镇), Lei Xia(夏雷), Ding Ding(丁鼎)**

Laboratory for Microstructure, Institute of Materials, Shanghai University, Shanghai 200072

(Received 29 August 2016)

Outstanding magneto-caloric properties of a $Gd_{60}Ni_{37}Co_3$ amorphous alloy are reported. The magnetic entropy change peak ($-\Delta S_m^{peak}$) near the Curie temperature ($T_c = 135\,K$) of the amorphous alloy under 5 T is about 10.42 $J{\cdot}kg^{-1}K^{-1}$ and the refrigeration capacity (RC) under 5 T is about 860 $J{\cdot}kg^{-1}$, both of which are almost the highest among the amorphous alloys with T_c above 100 K. The magneto-caloric behaviors and the mechanism for the rather high magneto-caloric effect of the $Gd_{60}Ni_{37}Co_3$ metallic glass are investigated.

PACS: 61.43.Dq, 81.05.Kf, 75.30.Sg, 81.20.−n DOI: 10.1088/0256-307X/33/12/126101

The magneto-caloric effect (MCE), discovered firstly by Warburg in 1881, is the lowering of entropy and the resulted heating of a magnetic material under a magnetic field due to the alignment of unpaired spin parallel to the magnetic field.[1–5] For decades, the MCE of magnetic materials has attracted a great deal of attention because a magnetic refrigeration (MR) cycle based on MCE has shown potential perspective as a new refrigeration technology superior to the traditional vapor compression-expansion cycle. Magnetic refrigerators using a solid working body show some advantages such as compactness, high effectiveness, low energy consumption and environmental safety. Therefore, the working materials for the MR technology have been intensively investigated and the number of MCE materials increases exponentially in recent years.

Among the MCE materials, metallic glasses could match most of the requirements for ideal magnetic refrigerants such as (1) a broadened magnetic entropy change peak ($-\Delta S_m$) and the resulted ultrahigh refrigeration capacity (RC) due to the second order magnetic phase transition they undergo, (2) ultralow hysteresis loss due to their negligible coercivity, (3) low eddy current loss due to their relatively high electric resistance, (4) tunable Curie temperature (T_c) within a large compositional range, and (5) rather high corrosion resistance and excellent mechanical properties.[6–14] However, the $-\Delta S_m$ peak values ($-\Delta S_m^{peak}$) of the metallic glasses are usually much lower than those of the intermetallic compounds such as $Gd_5(Si_2Ge_2)$, $MnFeP_{0.45}As_{0.55}$ and $Ni_{52.6}Mn_{23.1}Ga_{24.3}$, and both of them exhibit a sharp $-\Delta S_m$ peak due to their first order magnetic phase transition.[15–21] Thus the improvement of $-\Delta S_m^{peak}$ for the amorphous alloys becomes a key challenge for the industrial application of these MCE materials.

Recent results have shown that some of the Gd-based amorphous alloys exhibit $-\Delta S_m^{peak}$ close to or even higher than that of the pure Gd, and RC several times higher than that of the crystalline alloys.[8–14] Among these amorphous alloys, some of the Gd-Ni binary alloys can be fabricated into amorphous samples and show excellent MCE at temperatures above 120 K.[10,22] Based on these preliminary results, we fabricated Gd-Ni-Co binary amorphous alloys in an attempt to further improve T_c, $-\Delta S_m^{peak}$ and RC of the binary amorphous alloys. In the present work, we report a $Gd_{60}Ni_{37}Co_3$ amorphous alloy with outstanding magneto-caloric properties at the temperature around 135 K. The $Gd_{60}Ni_{37}Co_3$ amorphous alloy prepared by melt-spinning in the shape of a ribbon shows almost the highest $-\Delta S_m^{peak}$ and RC among the metallic glasses with the Curie temperature above 100 K. The magnetic properties as well as the magneto-caloric behaviors of the amorphous alloy are studied and the mechanism for the improved T_c and MCE by Co addition is investigated.

A $Gd_{60}Ni_{37}Co_3$ ingot was prepared by arc melting of 99.9 at.% pure Gd, Ni and Co elements, and was remelted four times in a watercooled copper crucible protected by a Tigettered argon atmosphere. The structure of the as-spun ribbons obtained by melt spinning on a single copper wheel with a linear surface speed of 30 m/s was checked by a Rigaku D/max2550 Xray diffractometer (XRD) using the Cu K_α radiation. A Perkin–Elmer diamond differential scanning calorimeter (DSC) and a NETZSCH DSC 404C high temperature DSC were used to measure the thermal properties of the as-spun ribbon at a heating rate of 20 K/min. The magnetic properties of the amorphous ribbons were measured by a Quantum Design 6000 physical properties measurement system (PPMS).

Figure 1 shows the XRD pattern of the $Gd_{60}Ni_{37}Co_3$ as-spun ribbon. The broad diffraction maxima in the XRD pattern illustrate the typical amorphous features of the $Gd_{60}Ni_{37}Co_3$ as-spun ribbons. The amorphous characteristics of the $Gd_{60}Ni_{37}Co_3$ as-spun ribbons were also ascertained by the glass transition and the crystallization behaviors in the DSC trace of the ribbon, as shown in the inset of Fig. 1. The onset temperature of glass transition (T_g) and the onset temperature of primary crystallization (T_x) marked clearly on the DSC trace of

*Supported by the National Natural Science Foundation of China under Grant Nos 51271103 and 51671119.

**Corresponding author. Email: d.ding@shu.edu.cn

© 2016 Chinese Physical Society and IOP Publishing Ltd

the $Gd_{60}Ni_{37}Co_3$ as-spun ribbon are about 568 K and 583 K, respectively. The melting behaviors of the ribbon were illustrated, as shown in the inset of Fig. 1. The melting temperature (T_m) and liquids temperature (T_l) of the ribbon, as marked on the high temperature DSC curve shown in the inset of Fig. 1, are about 961 K and 996 K, respectively. Therefore, the reduced glass transition temperature ($T_{rg} = T_g/T_l$) of the $Gd_{60}Ni_{37}Co_3$ glass forming alloy is about 0.57, indicating that the glass forming ability of the alloys is high enough so that it can be fabricated into amorphous ribbons easily.[23]

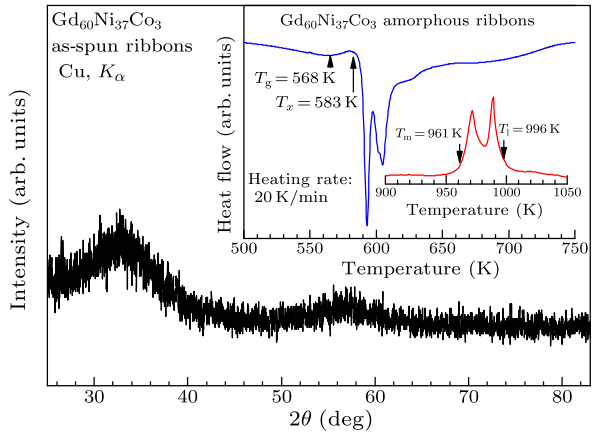

Fig. 1. XRD pattern of the $Gd_{60}Ni_{37}Co_3$ as-spun ribbon, and the inset is the DSC curves of the $Gd_{60}Ni_{37}Co_3$ amorphous ribbon at a heating rate of 20 K/min.

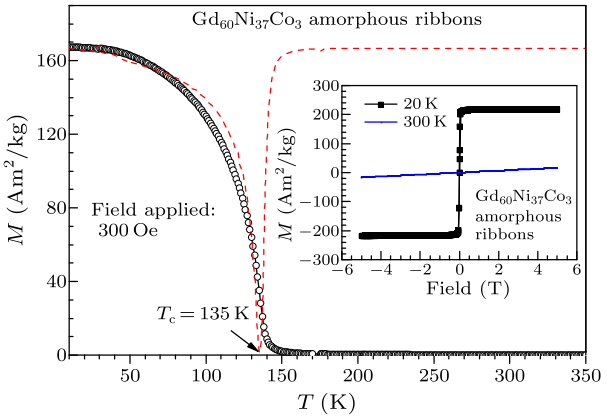

Fig. 2. The M–T curves of the $Gd_{60}Ni_{37}Co_3$ amorphous ribbon under a field of 0.03 T. The inset is the hysteresis loops of the $Gd_{60}Ni_{37}Co_3$ amorphous ribbon at 20 K and 300 K under a field of 5 T.

Figure 2 shows the temperature dependence of the magnetization (M–T) curve of the $Gd_{60}Ni_{37}Co_3$ as-spun ribbon measured under a field of 0.03 T from 10 K to 350 K after cooling from room temperature to 10 K under a zero magnetic field. From the derivative of the M–T curve (dashed line in Fig. 2), we can obtain T_c of the amorphous ribbon to be about 135 K, which is much higher than T_c of other Gd-Ni-based amorphous alloys.[10] The inset of Fig. 2 shows the hysteresis loops of the $Gd_{60}Ni_{37}Co_3$ amorphous ribbon measured under a magnetic field of 5 T at 20 K and 300 K, respectively. The amorphous ribbon is paramagnetic at room temperature and is soft magnetic at 20 K with a saturation magnetization (M_s) of about 217 Am^2/kg and a nearly zero coercivity (less than 4 kA/m) under a field of 5 T. The high saturation magnetization and negligible hysteresis of the $Gd_{60}Ni_{37}Co_3$ amorphous alloy at 20 K indicate the excellent MCE of the amorphous ribbons because either the magnetization or the magnetic entropy change of the magnetic materials depend mainly on the ordering of the magnetic moments.[8–14]

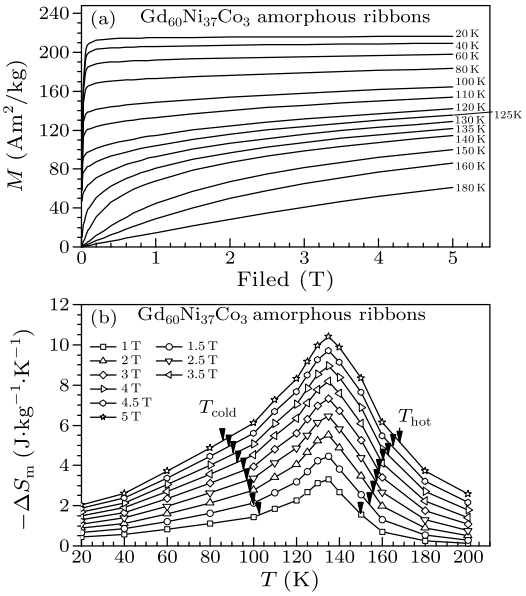

Fig. 3. (a) The isothermal magnetization curves of the $Gd_{60}Ni_{37}Co_3$ amorphous ribbon measured at various temperatures from 20 K to 200 K under a field of 5 T. (b) The $-\Delta S_m$–T curves under various magnetic fields of the $Gd_{60}Ni_{37}Co_3$ amorphous ribbon.

Figure 3(a) shows the isothermal magnetization (M–H) curves of the $Gd_{60}Ni_{37}Co_3$ amorphous ribbon measured at various temperatures from 20 K to 200 K under a field of 5 T. Thus the isothermal $-\Delta S_m$ curves under various magnetic fields can be derived from the isothermal magnetization curves according to the thermodynamic Maxwell equation as follows:

$$\Delta S_m(T,H) = S_m(T,H) - S_m(T,0) = \int_0^H \left(\frac{\partial S_m}{\partial H}\right)_T dH = \int_0^H \left(\frac{\partial M}{\partial H}\right)_T dH.$$

The temperature dependence of the magnetic entropy change [$(-\Delta S_m)$–T] curves under a field of 5 T for $Gd_{60}Ni_{37}Co_3$ is shown in Fig. 3(b). The broadened $-\Delta S_m$ peak of the amorphous ribbon, which is supposed to be resulting from the structural disorder of the material, reveals the typical characteristics of the magnets undergoing a second order magnetic phase transition. Here $-\Delta S_m^{peak}$ of the amorphous ribbon near T_c is about 3.3 $J\cdot kg^{-1}K^{-1}$ under 1 T, 4.47 $J\cdot kg^{-1}K^{-1}$ under 1.5 T, 5.51 $J\cdot kg^{-1}K^{-1}$ under 2 T, 6.45 $J\cdot kg^{-1}K^{-1}$ under 2.5 T, 7.34 $J\cdot kg^{-1}K^{-1}$ under 3 T, 8.17 $J\cdot kg^{-1}K^{-1}$ under 3.5 T, 8.95 $J\cdot kg^{-1}K^{-1}$ under 4 T, 9.7 $J\cdot kg^{-1}K^{-1}$

under 4.5 T, and 10.42 J·kg^{-1}K^{-1} under 5 T. On the other hand, as another important parameter evaluating the MCE of the magnetic materials, RC (=$-\Delta S_{\rm m}^{\rm peak} \times \Delta T_{\rm m}$, where $\Delta T_{\rm m}$ is the temperature range at the half maximum of the $-\Delta S_{\rm m}^{\rm peak}$) of the $Gd_{60}Ni_{37}Co_3$ amorphous ribbon can also be obtained from the $-\Delta S_{\rm m}$ curves to be about 144.4 J·kg^{-1} under 1 T, 224.3 J·kg^{-1} under 1.5 T, 303.9 J·kg^{-1} under 2 T, 391.8 J·kg^{-1} under 2.5 T, 479.1 J·kg^{-1} under 3 T, 566.7 J·kg^{-1} under 3.5 T, 665 J·kg^{-1} under 4 T, 762.4 J·kg^{-1} under 4.5 T, and 860 J·kg^{-1} under 5 T. Here $-\Delta S_{\rm m}^{\rm peak}$ and RC under different magnetic fields of $Gd_{60}Ni_{37}Co_3$ with other alloys was listed in Table 1. There are many GdNiCo ternary amorphous alloys that have been studied. We can see from Table 1, after adding the Co element, $-\Delta S_{\rm m}^{\rm peak}$ and RC make greater improvement than Gd-Ni amorphous alloys.[10] Thus adding the Co element can increase the prediction MCE effectively. Both $-\Delta S_{\rm m}^{\rm peak}$ and RC of the $Gd_{60}Ni_{37}Co_3$ amorphous alloy are almost the highest among the glassy alloys with $T_{\rm c}$ above 100 K, indicating the outstanding MCE of the $Gd_{60}Ni_{37}Co_3$ metallic glass.[10–13,20]

Table 1. The values of $-\Delta S_{\rm m}^{\rm peak}$ and RC under different magnetic fields of $Gd_{60}Ni_{37}Co_3$ and other alloys. A and C stand for amorphous and crystalline alloys, respectively.

Composition	Structure	$T_{\rm c}$ (K)	Applied field (T)	$-\Delta S_{\rm m}^{\rm peak}$ J·kg^{-1}K^{-1}	RC (J·kg^{-1})	References
$Gd_{60}Ni_{37}Co_3$	A	135	3	7.34	479.1	Present work
			5	10.42	860	
$Gd_{71}Ni_{29}$	A	122	5	9.0	724	Ref. [10]
$Gd_{68}Ni_{32}$	A	124	5	8.0	583	Ref. [10]
$Gd_{65}Ni_{35}$	A	122	5	6.9	524	Ref. [10]
$Gd_{50}Co_{50}$	A	267.5	5	4.6	685.9	Ref. [24]
$Gd_{71}Co_{29}$	A	166	1	3.1	92	Ref. [25]
$Gd_{55}Co_{20}Al_{25}$	A	112	5	9	541	Ref. [11]
$Gd_{60}Co_{25}Al_{15}$	A	125.5	5	9.97	860	Ref. [14]
$Gd_{50}Co_{45}Al_5$	A	197.5	5	6.64	764	Ref. [26]
$Gd_{50}Co_{48}Zn_2$	A	260	5	5.04	700	Ref. [27]
$Gd_{55}Co_{25}Ni_{20}$	A	140	5	6.47	502	Ref. [28]
$Gd_{55}Co_{30}Ni_{15}$	A	175	5	6.30	487	Ref. [28]
$Gd_{55}Co_{35}Ni_{10}$	A	192	5	6.04	450	Ref. [28]
$Gd_{55}Al_{20}Co_{20}Ni_5$	A	105	5	9.8	829	Ref. [29]
$Gd_{65}Fe_{10}Co_{10}Al_{10}B_5$	A	145	5	7.1	748	Ref. [30]
$Gd_{65}Fe_{10}Co_{10}Al_{15}$	A	160	5	6	700	Ref. [30]
$Gd_{65}Fe_{10}Co_{10}Al_{10}Si_5$	A	175	5	5.5	698	Ref. [30]
$Fe_{90}Zr_{10}$	A	230	5	2.7	497	Ref. [31]
$Fe_{88}Zr_8B_4$	A	280	5	2.8	551	Ref. [31]
$Gd_{15}Si_9C$	C	170	3	3.89	341	Ref. [32]
$Tb_{15}Si_9C$	C	135	3	6.50	163	Ref. [32]
Gd	C	293	5	9.7	556	Ref. [33]

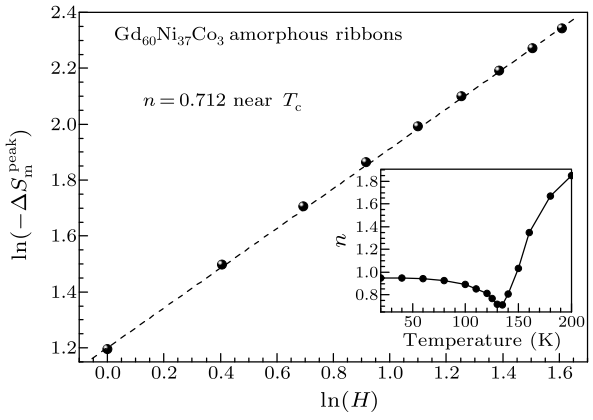

Fig. 4. The linear fitting for the $\ln(-\Delta S_{\rm m}^{\rm peak})$ vs $\ln(H)$ plots of the $Gd_{60}Ni_{37}Co_3$ amorphous ribbons. The inset is the n–T curve for the $Gd_{60}Ni_{37}Co_3$ amorphous ribbon.

The $-\Delta S_{\rm m}$ curves under various magnetic fields allow us to investigate the magneto-caloric behaviors of the $Gd_{60}Ni_{37}Co_3$ amorphous alloy in more details by constructing the field dependence of the $-\Delta S_{\rm m}$ ($-\Delta S_{\rm m} \propto H^n$) curve.[8,33–35] Figure 4 shows the linear fitting of the $\ln(-\Delta S_{\rm m}^{\rm peak})$ versus $\ln(H)$ plots of the $Gd_{60}Ni_{37}Co_3$ amorphous ribbons. The n value near $T_{\rm c}$ is about 0.712, which is larger than the theoretical one derived from the mean field theory while it is similar to the one predicted from the Arrott–Noakes equation.[22,23] The temperature dependence of n (n–T curve) for the amorphous alloy, as shown in the inset of Fig. 4, illustrates the typical magneto-caloric behaviors of fully amorphous alloys with local inhomogeneities: $n \approx 1$ at a temperature well below $T_{\rm c}$; n is close to 2 in the paramagnetic range as a consequence of the Curie–Weiss law; and $n = 0.712$ near $T_{\rm c}$.

The improved $T_{\rm c}$ and the simultaneously enhanced $-\Delta S_{\rm m}^{\rm peak}$ are anomalous because it is usually regarded that $-\Delta S_{\rm m}^{\rm peak}$ decrease with the improved $T_{\rm c}$ according to the linear relationship between $-\Delta S_{\rm m}^{\rm peak}$ and $T_{\rm c}^{-2/3}$ proposed from the mean field theory.[36] As we know, there are three kinds of interactions in the rare erath (RE)-transition metal (TM)-based alloys: the direct interaction between TM atoms, which governs $T_{\rm c}$ of the alloys; the indirect interactions between RE–TM and RE–RE atoms, both of which determine the

magnetic behaviors of the alloys. Therefore, the improved T_c of the $Gd_{60}Ni_{37}Co_3$ amorphous alloy is most likely due to the tradition of Co as a replacement of Gd, which results in the enhancement of the TM–TM interaction. On the other hand, the free electrons in transition metals act as an exchange interaction medium between $3d$ electrons and $4f$ electrons. Compared with Ni, the addition of a small amount of Co, with more unpaired $3d$ free electrons, will enhance the $3d$–$4f$ interactions,[21] and thus will improve the MCE of Gd-Ni amorphous alloys.

In summary, we have reported an outstanding MCE of a $Gd_{60}Ni_{37}Co_3$ amorphous alloy. The GFA of the $Gd_{60}Ni_{37}Co_3$ alloy is high enough so that it can be fabricated into amorphous ribbons. The $Gd_{60}Ni_{37}Co_3$ amorphous ribbons are paramagnetic at room temperature and soft magnetic at 20 K with an M_s of about $217\,Am^2/kg$ and a nearly zero coercivity under a field of 5 T. Here T_c obtained from the derivative of the M–T curve of the amorphous ribbon is about 135 K. The $Gd_{60}Ni_{37}Co_3$ amorphous alloy exhibits a rather high $-\Delta S_m^{peak}$ up to $10.42\,J{\cdot}kg^{-1}K^{-1}$ and an RC of about $860\,J{\cdot}kg^{-1}$ under 5 T, both of which are almost the highest among the amorphous alloys with T_c above 100 K. The magneto-caloric behaviors of the amorphous alloy are in accordance with those of other fully amorphous alloys with local inhomogeneities. The improved T_c as well as MCE of the $Gd_{60}Ni_{37}Co_3$ alloy are supposed to be induced by the enhanced exchange interaction by minor Co addition.

References

[1] Warburg E 1881 *Ann. Phys.* **13** 141
[2] Gschneider Jr K A, Pecharsky V K and Jr. and Tsokol A O 2005 *Rep. Prog. Phys.* **68** 1479
[3] Brück E 2005 *J. Phys.* D **38** R381
[4] de Oliveira N A and von Ranke P J 2010 *Phys. Rep.* **489** 89
[5] Tishin A M and Spichkin Y I **2003** *The Magnetocaloric Effect and Its Applications* (Bristol: Institute of Physics Publishing Ltd.)
[6] Franco V, Borrego J M, Conde A and Roth S 2006 *Appl. Phys. Lett.* **88** 132509
[7] Bingham N S, Wang H, Qin F, Peng H X, Sun J F, Franco V, Srikanth H and Phan M H 2012 *Appl. Phys. Lett.* **101** 102407
[8] Xia L, Chan K C, Tang M B and Dong Y D 2014 *J. Appl. Phys.* **115** 223904
[9] Luo Q, Zhao D Q, Pan M X and Wang W H 2006 *Appl. Phys. Lett.* **89** 081914
[10] Zhong X C, Tang P F, Liu Z W, Zeng D C, Zheng Z G, Yu H Y, Qiu W Q and Zou M 2011 *J. Alloys Compd.* **509** 6889
[11] Du J, Zheng Q, Li Y B, Zhang Q, Li D and Zhang Z D 2008 *J. Appl. Phys.* **103** 023918
[12] Xia L, Chan K C and Tang M B 2011 *J. Alloys Compd.* **509** 6640
[13] Yuan F, Du J and Shen B 2012 *Appl. Phys. Lett.* **101** 032405
[14] Xia L, Guan Q, Ding D, Tang M B and Dong Y D 2014 *Appl. Phys. Lett.* **105** 192402
[15] Pecharsky V K and Gschneider K A Jr 1997 *Phys. Rev. Lett.* **78** 4494
[16] Morellon L, Blasco J, Algarabel P A and Ibarra M R 2000 *Phys. Rev.* B **62** 1022
[17] Hu F, Shen B, Sun J, Wang G and Cheng Z 2002 *Appl. Phys. Lett.* **80** 826
[18] Fujita A, Fujieda S, Hasegawa Y and Fukamichi K 2003 *Phys. Rev.* B **67** 104416
[19] Hu F X, Shen B G, Sun J R and Wu G H 2001 *Phys. Rev.* B **64** 132412
[20] Stadler S, Khan M, Mitchell J, Ali N, Gomes A M, Dubenko I, Takeuchi A Y and Guimarães A P 2006 *Appl. Phys. Lett.* **88** 192511
[21] Wada H and Tanabe Y 2001 *Appl. Phys. Lett.* **79** 3302
[22] Li Z, Ding D and Xia L *unpublished data*
[23] Turnbull D 1969 *Contemp. Phys.* **10** 473
[24] Xia L, Wu C, Chen S H and Chan K C 2015 *AIP Adv.* **509** 7122
[25] Zhang C L, Wang D H, Han Z D, Xuan H C, Gu B X and Du Y W 2009 *Appl. Phys.* **105** 13912
[26] Wu C, Ding D and Xia L 2016 *Chin. Phys. Lett.* **33** 016102
[27] Yu P, Zhang N Z, Cui Y T, Wu Z M, Wen L, Zeng Z Y and Xia L 2016 *J. Non-Cryst. Solids* **434** 36
[28] Zhong X C, Tang P F, Liu Z W, Zeng D C, Zheng Z G, Yu H Y, Qiu W Q, Zhang H and Ramanujan R V 2012 *J. Appl. Phys.* **111** 07A919
[29] Xia L, Tang M B, Chan K C and Dong Y D 2014 *J. Appl. Phys.* **115** 223904
[30] Pierunek N, Sniadecki Z, Marcin J, Škorvánek I and Idzikowski B 2014 *IEEE Trans. Magn.* **50** 11
[31] Barandiaran J M, Gorria P, Orue I, Fdez-Gubieda M L, Plazaola F, Gomez Sal J C, Barquin L F and Fournes L 1997 *J. Phys: Condens. Mat.* **9** 5671
[32] Bhattacharyya A, Thamizhavel A, Dhar S K and Manfrinetti P 2014 *J. Alloys Compd.* **588** 720
[33] Shen J, Wu J F and Sun J R 2009 *J. Appl. Phys.* **106** 083902
[34] Franco V, Borrego J M, Conde C F, Conde A, Stoica M and Roth S 2006 *J. Appl. Phys.* **100** 083903
[35] Franco V, Blázquez J S and Conde A 2006 *Appl. Phys. Lett.* **89** 222512
[36] Bloe J H, Amaral J S, Pereira A M, Amaral V S and Araujo J P 2012 *Appl. Phys. Lett.* **100** 242407